

Low frequency dielectric permittivity of quasi-one-dimensional conductor (TMTTF)₂Br

F. Nad^{1,2}, P. Monceau^{1,a}, and J.M. Fabre³

¹ Centre de Recherches sur les Très Basses Températures, associé à l'Université Joseph Fourier, CNRS, BP 166, 38042 Grenoble Cedex 9, France

² Institut of Radioengineering and Electronics, Russian Academy of Sciences, Mokhovaya 11, 103907 Moscow, Russia

³ Laboratoire de Chimie Structurale Organique, Université de Montpellier, 34095 Montpellier Cedex 5, France

Received: 10 October 1997 / Revised: 28 February 1998 / Accepted: 3 March 1998

Abstract. Conductivity and permittivity ϵ of the organic transfer salt (TMTTF)₂Br have been measured at low frequencies (10^2 - 10^7 Hz) between room temperature down to 4 K. The real part of the permittivity, ϵ' , is shown to grow below the temperature T_ρ at which the conductivity is maximum due to charge localization of Mott-Hubbard type. ϵ' reaches a maximum of 10^5 - 10^6 at 35 K-50 K depending on the samples. Decreasing temperature below T_ρ , ϵ' sharply decreases down to helium temperature through the antiferromagnetic phase transition at $T_N = 15$ K. We explain the magnitude, the temperature and frequency dependence of ϵ' as resulting from short range charge density wave states in the temperature range where charge localization occurs. This interpretation is supported by recent X-ray scattering measurements.

PACS. 75.30.Fv Spin-density waves – 77.22.Gm Dielectric loss and relaxation – 71.30.+h Metal-insulator transitions and other electronic transitions

1 Introduction

Quasi-one-dimensional conducting cation-radical salts (TMTTF)₂X [TMTTF = tetramethyl-tetrathiafulvalene] and (TMTSF)₂X [TMTSF = tetramethyl-tetraselenafulvalene], where X = PF₆, Br, ClO₄ ..., show a large variety of electronic condensed states, including superconductivity, Spin Density Wave (SDW), antiferromagnetic, spin Peierls state, magnetic field induced SDW, *etc.* [1–3]. The possibility of realization of these states is essentially determined by electron-electron interactions, including correlated spin interaction. For this reason, probably, the majority of studies in this field have been dedicated to measurements of NMR, spin echo, magnetic susceptibility and so on.

However the question about the correlation between magnetic and charge properties of these quasi-one-dimensional conductors is very important. In many cases the synchronous variation of magnetic and electrical properties during the transition to above mentioned condensed states has been demonstrated. For example, when the selenides salts or Bechgaard salts as (TMTSF)₂PF₆, (TMTSF)₂NO₃, *etc.* undergo a transition into an incommensurate spin modulation state such as a Spin Density Wave (SDW), one can observe the change of magnetic

properties as well as the change of electrical characteristics with properties which are similar to those for systems with charge modulation-Charge Density Wave (CDW)-ground state. Thus, it was found a non-linear conductivity above a threshold field [4,5], narrow-band noise [6–8], memory effects, high dielectric susceptibility [9,10] and also the existence of frozen metastable states at low temperatures, which are characterized by the divergence of relaxation time and which are very similar to glassy state [11,12].

However, as it was shown by measurements in the sulfer salts, mainly in the case of formation of commensurate superstructures, magnetic and charge properties can be decoupled [2]. Charge localizations of Mott-Hubbard type occur in the (TMTTF)₂X salts in the range of 100-200 K, leaving unaffected the spin degrees of freedom [13]. Interchain exchange interaction between one-dimensional $2k_F$ spin fluctuations stabilizes a three-dimensional ordering antiferromagnetic state at low temperature. In (TMTTF)₂Br, this ordered state occurs at $T_N = 14$ K [2].

However, as far as we know, a detailed study of the appropriate variation of electrical properties of such materials in an extended temperature range has not been carried out up to now. Hereafter we present the results of detailed measurements of the complex conductivity and permittivity of (TMTTF)₂Br samples between room temperature down to helium temperature in the frequency range between 5×10^2 and 10^7 Hz.

^a e-mail: monceau@labs.polycnrs-gre.fr

2 Experimental

Crystals of $(\text{TMTTF})_2\text{Br}$ were prepared using standard electrochemical procedures [14]. Measurements were performed on samples with cross-section area $\sim 10^{-5} \div 10^{-4} \text{ cm}^2$ and length 3-6 mm. The samples were attached to gold wires (with diameter $17 \mu\text{m}$) by silver or gold paste which covered the whole area of sample ends, providing the homogeneous current distribution near contacts. It is known that cracks appear in the chains if the sample is cooled too fast [4]. However we did not observe any sizeable jumps of the sample resistance at the cooling rate $\sim 0.5 \text{ K}$ per minute. The measurements of real ($\Re\sigma$) and imaginary ($\Im\sigma$) parts of conductivity have been carried out by an impedance analyzer (HP 4192A) in the frequency range 5×10^2 - 10^7 Hz with the use of an additional preamplifier when at low temperatures the sample resistance became larger than $1 \text{ M}\Omega$ [15]. The amplitude of the ac electric field was chosen in such a range where the values of $\Re\sigma$ and $\Im\sigma$ were independent of the ac voltage amplitude.

3 Results

We have measured four samples of $(\text{TMTTF})_2\text{Br}$. Below we show the data for two samples with a conductivity at room temperature $\simeq 100 (\Omega\text{cm})^{-1}$, which is close to the value reported in [16]. By lowering temperature from room temperature, the conductivity first increases and reaches a maximum at $T_\rho = 225 \text{ K}$ for sample 1 and at 185 K for sample 2, then decreases down to the lowest temperature.

In Figure 1a we have drawn the temperature dependences of the real part of the conductance, G , measured at 10^4 Hz , as a function of the inverse temperature for samples 1 and 2, normalized to their maximum magnitude G_m . The steepest variation of G occurs near $T \simeq 100 \text{ K}$ as it can be seen by the first minimum of the temperature dependence of the logarithmic derivative shown in Figure 1b. The position of the minimum in $d\log(G)/d(1/T)$ variation is practically the same for both samples and is independent on frequency. In the temperature range between 100 K and 20 K , the decrease of G follows a thermally activated variation with an activation energy of $\simeq 75 \text{ K}$. In the temperature range between 300 K and 20 K , the conductivity is actually independent on frequency in our frequency domain up to 10^7 Hz . However, below $T \simeq 20 \text{ K}$, we have observed the beginning of a frequency dependence of $G(T)$ which becomes more pronounced at lower temperatures.

As can be seen from Figure 1a a sizeable peculiarity exists below 20 K on $G(1/T)$ dependences for both samples. The second minimum in the logarithmic derivative in Figure 1b at $T \simeq 15 \text{ K}$ corresponds to this peculiarity, at the same temperature for both samples and independent on frequency up to 10^7 Hz . This minimum in the logarithmic derivative is the signature of a temperature transition into the ordered antiferromagnetic state $T_N = 15 \text{ K}$, determined by measurements of spin susceptibility and spin relaxation [13]. In the temperature range 15 K - 8 K $G(1/T)$

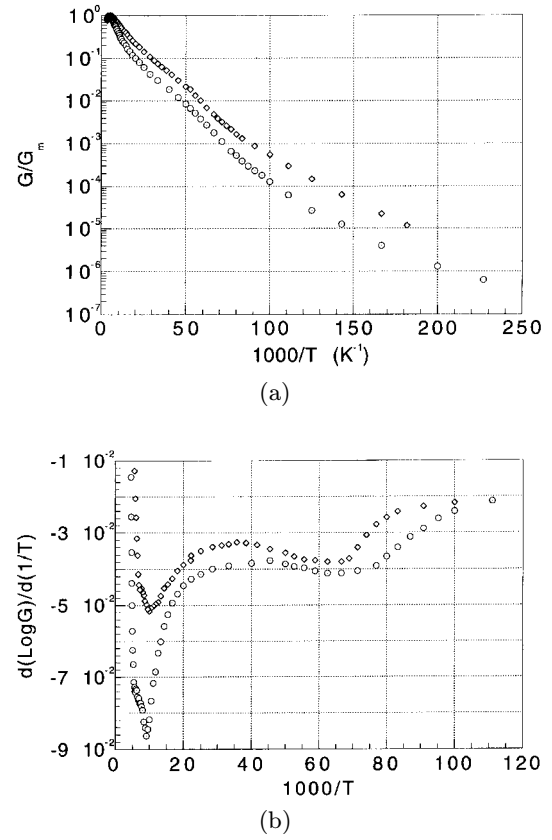


Fig. 1. (a) Variation of the real part of the conductance of $(\text{TMTTF})_2\text{Br}$ normalized to the maximum value measured at 10^4 Hz as a function of inverse temperature. Sample 1: \circ ; Sample 2: \diamond . (b) Temperature dependence of the logarithmic derivative of the conductance shown in Figure 1a for samples 1 and 2.

dependences are close to a thermally activated behaviour with an activation energy $\Delta_\ell \simeq 50 \text{ K}$ for both samples. This value is in good agreement with the gap value of the antiferromagnetic phase defined by $2\Delta = 3.5 kT_N$. Below $\sim 8 \text{ K}$ the $\log G(1/T)$ dependence deviates from linear to a sublinear variation.

The real ϵ' and imaginary ϵ'' parts of the dielectric permittivity have been calculated by standard equations: $\epsilon'(\omega) = \Im\sigma(\omega)/\omega$ and $\epsilon''(\omega) = \Re[\sigma(\omega) - \sigma_{dc}]/\omega$ [15]. Figure 2 shows the temperature dependence of $\epsilon'(T)$ of sample 2 at 1 MHz along with the temperature dependence of the conductivity at the same frequency.

Above T_ρ the dielectric permittivity is rather small. The scattering of the data above 200 K represents the resolution limit of our measurements of $\Im\sigma(\omega)$ with respect to the relatively large value of the $\Re\sigma(\omega)$ ($\simeq 10^{-3} \text{ S}$).

Below 190 K which practically corresponds to the temperature of the conductivity maximum at $T_\rho = 185 \text{ K}$, the magnitude of ϵ' begins to grow reaching the maximum value of $\epsilon' = 1.7 \times 10^5$ at $T = 35 \text{ K}$ for sample 2. The temperature dependence of ϵ' for sample 1 is similar with a maximum value of 7×10^5 near 50 K .

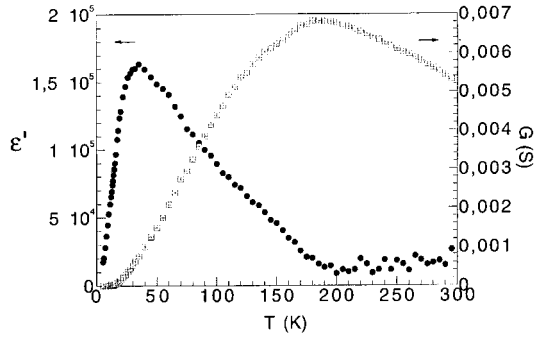


Fig. 2. Temperature dependence of the real part of the dielectric permittivity ϵ' (\bullet) and of the conductivity (\boxplus) of (TMTTF)₂Br (sample 2) measured at 1 MHz.

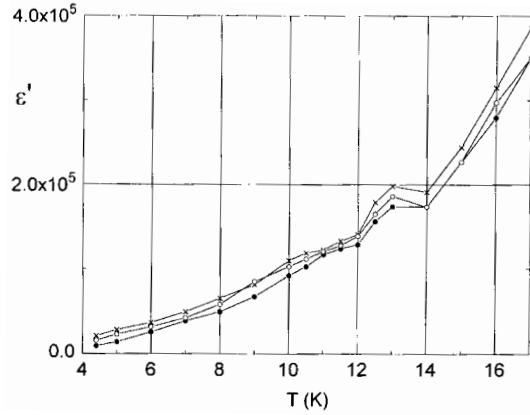


Fig. 3. Temperature dependence of the real part, ϵ' , of the dielectric permittivity of (TMTTF)₂Br (sample 1) in the low temperature range at frequencies (in kHz): \times - 1, \circ - 2, \bullet - 5.

Below this maximum ϵ' decreases sharply down to the value of 10^4 at liquid helium temperature. However a small peculiarity is observed in the $\epsilon(T)$ dependence near T_N more pronounced as frequency is decreased as shown in Figure 3. The position of this peculiarity on the temperature scale does not depend on frequency.

Figure 4 shows the frequency dependences of real part of conductivity $\Re\sigma(\omega)$ at different temperatures for sample 1. In the temperature range 20-8 K $\Re\sigma(\omega)$ is practically independent on frequency at low frequencies and its value corresponds to σ_{dc} value. The growth of $\Re\sigma(\omega)$ begins above some frequency, the value of which decreases with decreasing temperature. Below 8 K, $\Re\sigma(\omega)$ does not approach a constant value down to the lowest frequency of our measurements (5×10^2 Hz). Such a type of behaviour is typical for some disordered materials for which hopping conductivity dominates [15,18]. At enough low temperatures the frequency dependent conductance for these materials exhibits a power-law dependence as: $\Re G(\omega) \sim \omega^s$. As can be seen in Figure 4, the real part of the conductance, G , at $T = 4.4$ K do not completely follow this law, which would be probably the case at lower temperatures. However, using the high frequency part ($f > 10^5$ Hz) of $G(\omega)$ at $T = 4.4$ K, one can evaluate the exponent $s = 0.38 \pm 0.02$.

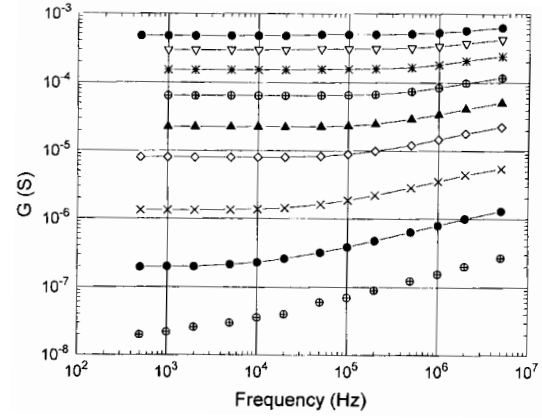


Fig. 4. Frequency dependence of the real part of the conductance of (TMTTF)₂Br (sample 1) at temperatures (K): \oplus - 4.4; \bullet - 6; \times - 8; \diamond - 10; \blacktriangle - 12; \oplus - 14; $*$ - 16; ∇ - 18; \bullet - 20.

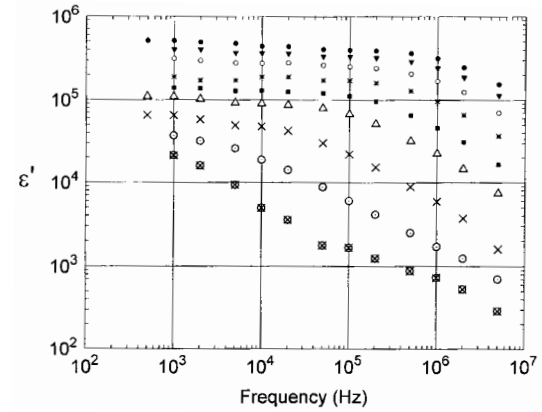


Fig. 5. Frequency dependence of the real part, ϵ' , of the dielectric permittivity of (TMTTF)₂Br (sample 1) at temperatures (K): \otimes - 4.4; \odot - 6; \times - 8; \triangle - 10; \blacksquare - 12; $*$ - 14; \circ - 16; \blacktriangledown - 18; \bullet - 20.

Figure 5 shows the frequency dependences of $\epsilon'(\omega)$ at various temperatures in the range 4.4-20 K. At 4.4 K the $\epsilon'(\omega)$ dependence is close to a power-law dependence $\epsilon' \sim \omega^{-n}$. However, the scattering of data because the ϵ' values are not far from the resolution limit of our experimental set up cannot allow a precise determination of the exponent n . It is more appropriate to use the high frequency data at a slightly higher temperature where the scattering of data is smaller. Thus at $T = 6$ K for $f > 10^4$ Hz one obtains: $n = 0.58 \pm 0.02$.

At higher temperatures $\epsilon'(\omega)$ consists of two approximately linear sections in the logarithmic scale: at low frequencies ϵ' depends very weakly on frequency, at high frequencies $\epsilon' \sim \omega^{-n}$ with approximately the same value of n as at low temperatures. The crossover between these two sections shifts to higher frequency with increasing temperature and the $\epsilon'(\omega)$ dispersion decreases. With increasing temperature from 4.4 K up to 30 K the ϵ' magnitude grows monotonously at all frequencies under investigation.

The frequency dependences of $\epsilon''(\omega)$ shown in Figure 6 in a double logarithmic scale present a qualitative

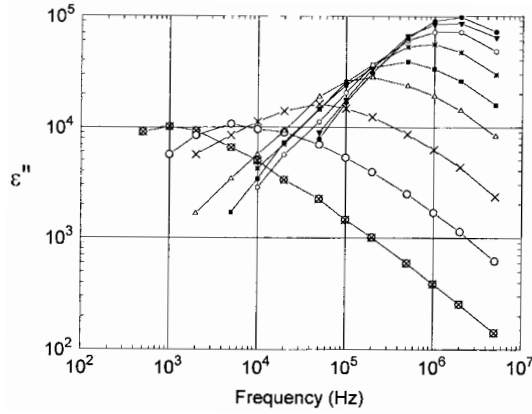


Fig. 6. Frequency dependence of the imaginary part, ϵ'' , of the dielectric permittivity of $(\text{TMTTF})_2\text{Br}$ (sample 1) at temperatures (K): \otimes - 4.4; \odot - 6; \times - 8; \triangle - 10; \blacksquare - 12; $*$ - 14; \circ - 16; \blacktriangledown - 18; \bullet - 20.

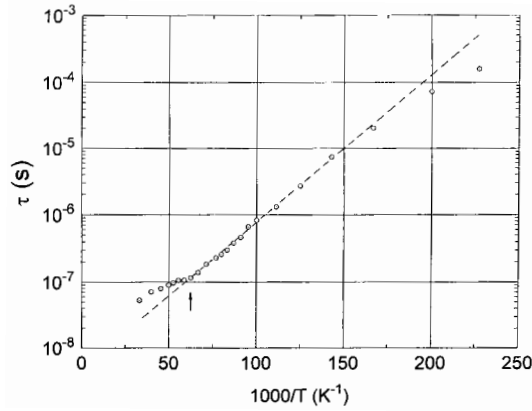


Fig. 7. Temperature dependence of the relaxation time of dielectric relaxation of $(\text{TMTTF})_2\text{Br}$ (sample 1). The dashed line corresponds to the thermally activated behaviour with activation energy of ≈ 50 K. The arrow indicates the antiferromagnetic transition at $T_N \approx 15$ K.

similarity at different temperatures. The $\epsilon''(\omega)$ curves at different T can be brought into coincidence by a shift along the two coordinate axis. With increasing temperature the $\epsilon''(\omega)$ maxima shift to high-frequency range. In the frequency range above the frequency f_m of the $\epsilon''(\omega)$ maximum, the variation of ϵ'' versus frequency has the form $\epsilon'' \sim \omega^{-m}$, where $m \approx 0.58$. In accordance with well-known equations [18] for Debye-type relaxation the reciprocal frequency, f_m , corresponds to some average relaxation time $\tau = 1/2\pi f_m$. At each temperature f_m has been determined by differentiation of the $\epsilon''(\omega)$ curves. Figure 7 shows the temperature dependence of $\tau(1/T)$ obtained on the basis of this equation. As can be seen from Figure 7 in the temperature range 4.4-15 K this dependence is close to an activated form $\tau \sim \tau_0 \exp(E/T)$ with $\tau_0 \approx 5 \times 10^{-9}$ s and $E \sim 50$ K. Near 15 K we can see a bend on the $\tau(1/T)$ dependence with a reduced slope at higher temperatures.

4 Discussion

The different temperature intervals for $(\text{TMTTF})_2\text{Br}$ ground states with decreasing temperature have been considered in a number of publications [2, 3, 13, 16].

Two main regions can be distinguished according to the temperature dependences of conductivity and dielectric response: $T_N < T \leq T_\rho$ and $T \leq T_N$. In the temperature region above T_N the temperature dependence of conductivity is characterized by the existence of a maximum with a thermally activated behaviour which can be considered as an evidence for a transition into some ground state at $T < T_\rho$; so the temperature $T_\rho^* \approx 100$ K of the first minimum in the logarithmic derivative of conductivity (Fig. 1b) can be considered as the “critical” temperature of such a transition. The electrical conductivity of the ground state is determined by the existence of some degree of dimerization in chains of $(\text{TMTTF})_2\text{Br}$ [19, 20], which is especially important in the case of predominance of one-dimensional intrachain interaction. As a result, the so-called dimerized gap can be opened in the spectrum of electron excitations [19, 20]. Simultaneously with decreasing conductivity the another fundamental physical parameter of the material — the dielectric permittivity ϵ' — shows a monotonous growth beginning at a temperature close to T_ρ (Fig. 2). The $\epsilon'(T)$ magnitude approaches a high value in the order of 10^5 - 10^6 at a maximum near 35 K followed by an abrupt decrease. It should be noted that half of this ϵ' decrease occurs at the critical temperature $T_N \approx 15$ K. At the same temperature the $d(\log \sigma)/d(1/T)$ dependence shows the second minimum (Fig. 1b) which identifies T_N as a transition into a new ground state.

The $\epsilon'(T)$ dependence (Fig. 2) is qualitatively similar to the temperature dependence of the $2k_F$ peak intensity of X-ray diffuse scattering recently reported [20] in $(\text{TMTTF})_2\text{Br}$. The difference in temperatures for the beginning of growth of the structural peak intensity and growth of ϵ' , as well as the appropriate difference in temperatures of their maxima, can be probably ascribed to difference in sample quality (for example defect concentration), as well as the absence of direct proportionality between the X-ray peak intensity and magnitude of ϵ' . However it is more important to underline the main qualitative similarity between these dependences. Taking into account the results of X-ray diffuse scattering [20] with respect to our permittivity measurements, we believe that the growth of ϵ' is due to fluctuations of a $2k_F$ dispersive lattice instability of spin-Peierls type which develops at $T < T_\rho$. But a real $2k_F$ superstructure with a finite gap does not condense because it is hindered by thermal fluctuations. Then, the large ϵ' magnitude in response to an ac field corresponds probably to some fluctuating charge density wave. The simultaneous growth of ϵ' and of X-ray diffuse scattering with decreasing temperature are due to the relative weakening of thermal fluctuations and improvement of the $2k_F$ ordering.

With a subsequent decrease of temperature, the interchain interaction and three dimensional effects begin to play an important role [2, 3]. At $T_N = 15$ K, $(\text{TMTTF})_2\text{Br}$ undergoes gradually a transition into an antiferromagnetic

spin ordering as revealed by many experiments as spin susceptibility [13]. The suppression of the $2k_F$ fluctuations and the decrease of ϵ' begin in the same temperature range above T_N . Near and below T_N these fluctuations decrease but remain observable down to ≈ 10 K [20]. As can be seen in Figures 2 and 5, the magnitude of ϵ' in the same temperature range becomes also smaller but still with a finite measurable magnitude. It seems that in this temperature range a finite charge modulation still exists or that the application of an electric field may induce a finite polarization. A similar situation is probably realized in the Bechgaard salt (TMTSF)₂PF₆ where, in accordance to recent results [19,20], the ground state in the spin ordered phase is characterized by the existence of a mixture of SDW and CDW. More precisely it consists of two CDW's of opposite spin with an arbitrary phase [21]. In (TMTTF)₂Br, in spite that the antiferromagnetic ground state becomes commensurate with the pristine lattice at $T = T_N$, small $2k_F$ CDW fluctuations remain below T_N [20]. The dielectric response we have measured in this temperature range with a finite value of ϵ' can be associated with the gradually reduced contribution of these $2k_F$ fluctuations. Simultaneously $4k_F$ satellites have been observed at $T < T_N$ [20], which are due to the magnetoelastic coupling of the lattice with the antiferromagnetic modulation, as typical for many antiferromagnets. Such $4k_F$ lattice displacement wave can lead to the appropriate charge modulation *i.e.* to $4k_F$ CDW which can also give some contribution to the dielectric response of (TMTTF)₂Br at $T < T_N$.

Our results for $\sigma(\omega, T)$, $\epsilon'(\omega, T)$, $\epsilon''(\omega, T)$ and $\epsilon(T)$ (Figs. 4-7) in the temperature range $T \leq T_N$ show a behavior similar to that measured in other CDW systems at low temperature [15]. Indeed, the temperature dependences of $\Re G(\omega)$ of (TMTTF)₂Br (Fig. 4) at $T < T_N$ have similar features with those measured in CDW one-dimensional conductors such as TaS₃ at $T < T_P/2$ [15]. At low temperature, the $G(\omega)$ dependences correspond to the equation $G(\omega) \sim \omega^n$, which is characteristic for variable range hopping mechanism of conductivity in disordered systems [17,18]. The variation of $\epsilon'(\omega, T)$ and $\epsilon''(\omega, T)$ with frequency and temperature and the possibility of scaling between them in log ω scale are also similar to appropriate dependences observed in TaS₃ [15]. At very low temperature (in our case for (TMTTF)₂Br, below 4.4 K) when the variable range hopping mechanism for conductivity becomes dominant, hops of electrons as well as hops of the collective CDW excitations (soliton type) between metastable states have been shown to contribute to the conductivity [22-24]. As described in [18], these processes contribute not only in the real part of conductivity *i.e.* in ϵ'' , but also in the imaginary part *i.e.* in ϵ' .

Below T_N , the relaxation time of charge excitations τ grows exponentially with $E \simeq 50$ K, a value close to the activation energy of the electrical conductivity in the same temperature range (Fig. 1). Such a behavior is also analogous to the appropriate $\tau(1/T)$ variation measured in quasi-one-dimensional CDW conductors in the intermediate temperature range around $T_P/2$; it is associated with the reduction of the number of free electrons which

lead to the slowing down of the CDW excitations and consequently to the growth of the relaxation time. However, in (TMTTF)₂Br the frequency dependent maxima in the $\epsilon'(T)$ curves and the divergent branch on $\tau(1/T)$ dependence [11,12] measured in TaS₃ at very low temperature ($T < 50$ K) are absent. This is probably due to the smaller degree of charge modulation in (TMTTF)₂Br samples in comparison with pure CDW quasi-one-dimensional conductors of TaS₃ type. In such a structure close to commensurability with a weak charge modulation, the formation of collective CDW excitations, such as solitons, dislocations, discommensurations, needs an energy of the order of the lattice distortion gap which is not favorable. In this case the absence of the above mentioned $\epsilon'(T)$ maxima and $\tau(\frac{1}{T})$ divergence is consistent with our model for density wave conductors [11,12,15], in which these collective CDW excitations and the interaction between them determine the tendency towards a glass transition with a diverging τ at a finite temperature.

5 Conclusions

The behaviour of the quasi-one-dimensional organic conductor (TMTTF)₂Br with intermediate degree of stack dimerization cannot be reduced to only two ground states: charge localization at $T_N < T < T_\rho$ and antiferromagnetic state at $T < T_N$. According to the recent discovery of $2k_F$ X-ray diffuse scattering at $T < T_N$ and T near T_N and in addition of $4k_F$ satellite reflections at $T < T_N$ [20], a charge modulation exists in (TMTTF)₂Br, which corresponds as a matter of fact to the formation of appropriate CDW states. The large magnitude of ϵ' (up to 10^6), its dependence on temperature and frequency manifest the existence of such CDW states in (TMTTF)₂Br.

However at low temperatures below T_N the degree of charge modulation seems to be not very large (in this temperature range $\epsilon' \sim 10^4 - 10^5$), probably due to the closeness of the two-fold commensurability. In such a case the number of CDW collective excitations is small and the interaction between them weak (the CDW phase mode becomes weaker). As a result the tendency of growth of coherence length and dielectric permittivity at low temperatures observed in incommensurate density wave conductors [11,12,15] turns out to be blocked.

We thank J. Bret for help in the experiments. One of us (F.N.) is thankful to the CRTBT for kind hospitality during his stay in Grenoble. Part of this work was supported by the Russian Fund for Fundamental Research (grant N 95-03-05811), and the program PICS n° 153 from CNRS.

References

1. G. Grüner, Rev. Mod. Phys. **66**, 1 (1994).
2. D. Jérôme, Solid State Commun. **92**, 89 (1994); C. Bourbonnais, Synth. Met. **84**, 19 (1997).
3. D. Jérôme *et al.*, Synth. Met. **70**, 719 (1995).

4. S. Tomić, J.R. Cooper, D. Jérôme, K. Bechgaard, Phys. Rev. Lett. **62**, 462 (1989); S. Tomić, J.R. Cooper, W. Kang, D. Jérôme, K. Maki, J. Phys. I France **1**, 1603 (1991).
5. T. Sambongi *et al.*, Solid State Commun. **72**, 817 (1989).
6. K. Nomura *et al.*, Solid State Commun. **72**, 1123 (1989).
7. N. Hino *et al.*, Synth. Met. **40**, 275 (1991).
8. G. Kriza *et al.*, Phys. Rev. Lett. **66**, 1922 (1991).
9. G. Mihaly, Y. Kim, G. Grüner, Phys. Rev. Lett. **66**, 2806 (1991).
10. J.L. Musfeldt, M. Poirier, P. Batail, C. Lenoir, Phys. Rev. B **51**, 8347 (1995).
11. J.C. Lasjaunias, K. Biljaković, F. Nad', P. Monceau, K. Bechgaard, Phys. Rev. Lett. **72**, 1283 (1994).
12. F. Nad', P. Monceau, K. Bechgaard, Solid State Commun. **95**, 655 (1995).
13. P. Wzietek *et al.*, J. Phys. I France **3**, 171 (1993).
14. P. Delhaes, C. Coulon, J. Amiell, S. Flandrois, E. Tororeilles, J.M. Fabre, L. Giral, Mol. Cryst. Liq. Cryst. **50**, 43 (1979).
15. F. Nad', P. Monceau, Phys. Rev. B **51**, 2052 (1995).
16. S. Tomic, N. Biškup, S. Dolanski Babić, K. Maki, Europhys. Lett. **26**, 295 (1994); M. Basletić, D. Zanchi, B. Korin-Hamzić, A. Hamzić, S. Tomić, J.M. Fabre, J. Phys. I France **6**, 1855 (1996).
17. N.F. Mott, E.A. Davis, *Electron Processes in Non-Crystalline Materials* (Clarendon Press, Oxford, 1979).
18. A.K. Jonscher, *Dielectric Relaxation in Solids* (Chelsea, London, 1983).
19. J.P. Pouget, S. Ravy, J. Phys. I France **6**, 01 (1996).
20. J.P. Pouget, S. Ravy, Synth. Met. **85**, 1523 (1997).
21. A.W. Overhauser, Phys. Rev. **167**, 691 (1968).
22. M.E. Itkis, F.Ya. Nad', P. Monceau, J. Phys.: Condens. Matter **2**, 8327 (1990).
23. F.Ya. Nad', JETP Lett. **58**, 107 (1993).
24. A.I. Larkin, JETP **78**, 971 (1994).